April, 1981

Interferometer studies of equatorial Fregion irregularities and drifts

E. Kudeki
Bela G. Fejer, *Utah State University*
D. T. Farley
H. M. Ierkic

GEOPHYSICAL RESEARCH LETTERS, VOL. 8, NO. 4, PAGES 377-380, APRIL 1981

INTERFEROMETER STUDIES OF EQUATORIAL F REGION IRREGULARITIES AND DRIFTS

E. Kudeki, B. G. Fejer, D. T. Farley and H. M. Ierkic*

School of Electrical Engineering, Cornell University, Ithaca, NY 14853

Abstract. A radar interferometer technique developed at Jicamarca, Peru and first used to study electrojet irregularities has now been used successfully to study plasma turbulence in the equatorial F region. Our first results have shown that the most 'turbulent' echoes appear to come from a region that extends for tens of kilometers in altitude but for only a kilometer or less in the east-west direction. This slab may very well be the wall of a depleted region, a plasma 'bubble'. Sometimes the irregularities can be tracked as they move eastward or westward. Velocity profiles for the evening period obtained in this way show a strong shear, with westward velocities at the lowest altitudes observed and eastward velocities above. A plausible explanation for this shear is that the westward drifts are driven by electric fields produced by westward E region winds and mapped up along magnetic field lines, while at higher heights, where the electron density is greater, the drifts are controlled by the F region dynamo driven by eastward winds.

Introduction

The radar interferometer that was first used at the Jicamarca Radio Observatory in Peru to study the nighttime equatorial electrojet irregularities [Farley et al., 1981] can also be used effectively to study equatorial F region irregularities, often called spread F irregularities, with excellent spatial resolution. With an east-west baseline, the location of small patches of irregularities in the east-west plane can be determined to within a small fraction of the width of the scattering volume determined by the antenna beamwidth. Hitherto unobservable features of the plasma turbulence in the F region can be studied. It is also often possible to track the east-west motion of the irregularities and thereby determine a drift velocity profile. Normal east-west drift measurements at Jicamarca are made using incoherent scatter [Woodman, 1972; Fejer et al., 1981] and averaging the data over about 100 km in altitude near the F region peak, but incoherent scatter measurements cannot be made when strong spread F is present. Fortunately, this is just the time when the interferometer method we are discussing here works best, and furthermore we can often determine the drift velocity far below the F region peak, since strong irregularities are often present in this 'valley' region. Our measurements in the post-sunset period clearly show a large velocity shear with eastward velocities throughout most of the F region and westward velocities below. Ion cloud drift data [Valenzuela et al., 1981] and some very recent radar observations at Kwajalein [Tsunoda et al., 1981] also suggest a shear, but our results show this feature in detail.

Experimental Procedures

The measurement is essentially the same as that described by Farley et al. [1981] for the E region. The full large 50 MHz incoherent scatter antenna at Jicamarca (11°57'S, 76°52'W; magnetic dip 2°N) was used for transmission, and the east and west quarters were used separately for reception. In this configuration, the scattering volume is determined by the main lobe of the antenna (beamwidth about 1.2°) and the pulse length of 33 μsec. The height resolution was thus 5 km, and 32 heights were sampled over a range of 160 km centered in the region of strongest spread F echoes. The interpulse period (IPP) was 8 msec, which allowed Doppler shifts of up to ±62.5 Hz to be measured without aliasing.

Fourier transforms of the digitized signals from the east and west antennas, $F_E(\omega)$ and $F_W(\omega)$, were used to compute an estimate of the complex normalized cross spectrum (NCS):

$$S_{EW}(\omega) = \frac{\langle F_E(\omega) F_W^*(\omega)\rangle}{\langle |F_E(\omega)|^2\rangle^{\frac{1}{2}} \langle |F_W(\omega)|^2\rangle^{\frac{1}{2}}} \qquad (1)$$

where the angular brackets indicate ensemble averaging. For each Doppler frequency, ω, S_{EW} can be described by its magnitude or coherence $|S|$ and its phase angle Φ. For scatterers small compared to the scattering volume, the coherence and phase angle are given by [Farley et al., 1981]:

$$|S| = e^{-\frac{1}{2}k^2D^2\sigma_\omega^2} \qquad (2)$$

$$\Phi = kD\overline{\theta}_\omega \qquad (3)$$

where k is the radar wavenumber, D is the distance between the phase centers of the two antennas (34.65 wavelengths in this case), σ_ω is the angular size of the scatterer, and $\overline{\theta}_\omega$ is the zenith angle indicating the mean position of the scatterer in the east-west plane. At a given Doppler shift ω, the coherence is high (close to unity) when there is only a single small localized scatterer in the scattering volume, in which case the angular position of the scatterer in the east-west plane (for an east-west baseline) can be determined from the phase angle. Changes in the phase angle with time determine an east-west velocity, while the Doppler shift ω determines the radial (vertical) velocity. For diffuse scattering regions the coherence is small. More complete discussions of this radar interferometry

*Now at Max-Planck-Institut fur Aeronomie, Postfach 20, D-3411 Katlenburg-Lindau 3, West Germany.

Paper number 1L0319.
0094-8276/81/001L-0319$01.00

are given by Ierkic [1980] and Farley et al. [1981].

Results and Discussion

Spectra and cross spectra. Three sets of spectral data, illustrating the variety of results that are obtained, are shown in Figure 1. The power spectra (labeled P) are similar to those obtained by Woodman and LaHoz [1976]. The new cross-spectral information is shown as coherence $|S|$ and phase angle Φ. The top set of data shows that sometimes echoes with narrow, single peaked Doppler spectra have low coherence, meaning that echoes with essentially the same Doppler shift (vertical phase velocity) are coming from a range of east-west positions within the scattering volume. It is quite likely that the mean Doppler shift in the top set corresponds to the mean motion of the layer, in which case the echoes correspond to quite small turbulent velocities.

The middle data set of Figure 1 shows spectra with narrow multiple peaks and high corresponding coherence values, even for the relatively weak peaks. Furthermore, the phase angles corresponding to the several peaks are nearly the same, implying that although the scattering centers have different radial velocities (giving different Doppler shifts), they are located very close together. For example, a 30° phase increase (one tic mark) corresponds to an eastward displacement of 1.23 km at 510 km.

In the final (bottom) set of data this localization is even more pronounced. The spectra are broad and multipeaked and possibly aliased, implying strongly turbulent motion. The signal level was of the order of 30 dB above noise; hence even the minima in the spectra are far above incoherent scatter levels. The phase data show that all the scattered signal came from field aligned irregularities within a region that was no more than about 1 km in east-west extent. During these observations similar power and normalized cross spectra were obtained from an altitude range covering 50 km, although at some heights the phase angles were more spread than those shown for 500 km. These data imply that the scattering region was shaped like a thin (in the east-west direction) wavy wall extending tens of kilometers in altitude. Since the irregularities are known to be highly field aligned, they must also extend a considerable distance along

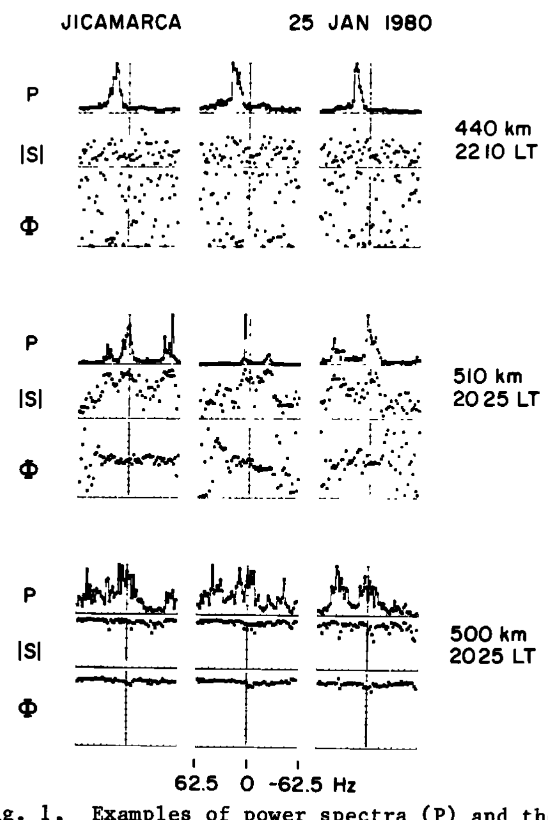

Fig. 1. Examples of power spectra (P) and the coherence ($|S|$) and phase angle (Φ) of the corresponding cross spectra obtained from the interferometer. Each individual example represents 5.12 s of integration, which is also the separation between the three examples in each set. The power spectra are normalized to a maximum value of unity, the coherence is $\leq$ 1, and the phase angle scale covers 360° (each tic mark is 30°). The last two quantities are described by (1) - (3) in the text.

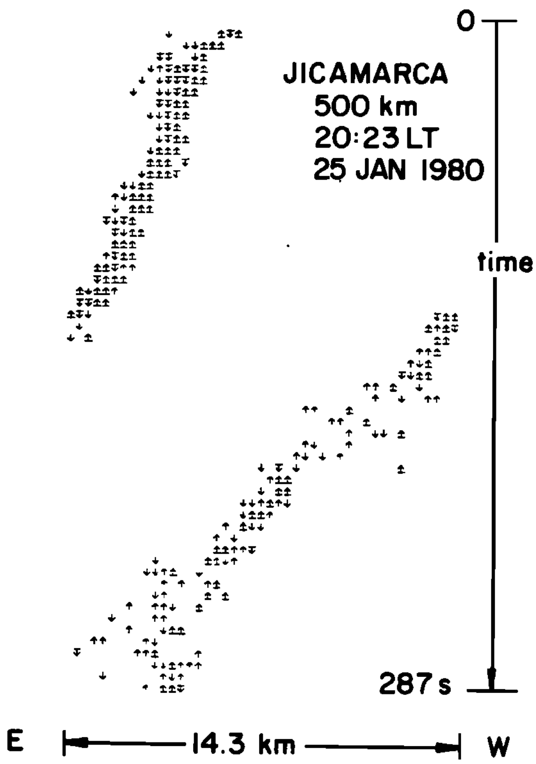

Fig. 2. The position in the east-west plane of localized scatterers with coherence $\geq$ 0.7 as a function of time. The direction of the arrows indicates the sense of the vertical Doppler velocity and a tail on the arrow means the velocity is greater than 93 m/s. The positions are determined from the phase of the cross spectrum (see Figure 1), which is why the apparent position 'wraps around' as the irregularity patch continues to drift eastward. The (local) starting time of these observations was 2023.

the magnetic field lines. It is certainly tempting to associate this region with the highly structured plasma 'bubble' walls, with sharp gradients of both signs separated by distances often less than 100 m, that have been detected by rockets and satellites [M. Kelley, private communication, 1980]. This idea also fits the observations of Woodman and LaHoz [1976], who reported that broad multipeaked power spectra with large Doppler shifts were usually associated with 'plumes' in their range-time-intensity plots.

East-West Drifts. As mentioned previously, the east-west drift velocity of the background plasma can be estimated by measuring the time dependence of the phase angle of discrete scatterers in the echoing region. The same procedure was used successfully by Farley et al. [1981] to measure the height variation of the east-west drift velocity of the electrons in the equatorial electrojet during nighttime. The drift velocities can be estimated only at heights where the scatterers are localized, which is not always the case in the F region, as we have seen. Nevertheless, in many instances we were able to estimate the velocity at enough heights to determine the profile.

The motion of discrete scatterers can be clearly visualized by plotting their position in the east-west plane as a function of time, as shown in Figure 2. The arrows indicate the vertical wave velocity. The scatterers represented in Figure 2 correspond to the echoing slab discussed in the previous section. The space and time coordinates of the scatterers are organized in 'streaks' which represent the motion of the scattering region. For the example shown in Figure 2 the drift velocity obtained from the slope of the streak is eastward with a magnitude of about 60 m/sec. Note that the position of the scattering region 'wraps around' in Figure 2, due to the usual 2π ambiguity in any phase measurement, and can be followed for almost 20 km of eastward motion. This is considerably more than the two-way half-power antenna beamwidth at 500 km; it is about the 20 dB beamwidth, in fact. It is because the echoes are so strong that the irregularities sometimes can be tracked so far. The side lobes in the east-west plane of the two-way pattern are down more than 30 dB and can be neglected.

From data such as those shown in Figure 2, we can determine a profile of drift velocity, which is presumably the velocity of the background plasma. Figure 3 shows four profiles, each derived from about 6 min of data. An obvious feature is the large shear, with westward motion in the lower part of the profile and eastward motion above. Ion cloud release experiments conducted at various locations [Valenzuela et al., 1981] have also shown such shears, and unpublished Jicamarca observations of spread F using multiple beams have indicated westward drifts on the bottom side of the F layer during evening hours [J.P. McClure, private communication, 1980]. Indications of this effect have also been seen at Kwajalein [Tsunoda et al., 1981]. We suspect that this shear is a regular feature of equatorial dynamics because previous east-west drift measurements using incoherent scatter observations have shown little variation with season, solar cycle, or magnetic activity [Woodman, 1972; Fejer et al., 1981], and the magnitude and direction of the drifts measured with the interferometer near the F region peak agree well with the incoherent scatter drift data.

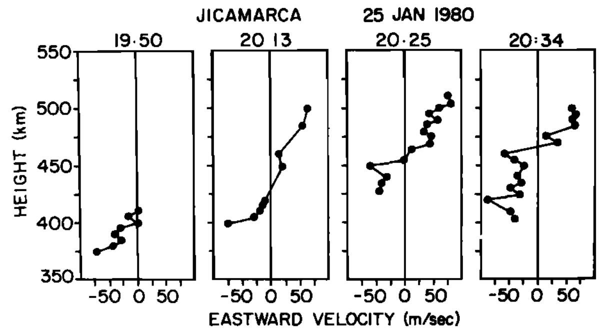

Fig. 3. Drift velocity profiles derived from the slopes of 'streaks' such as those shown in Figure 2. Each profile represents an average of about 6 min. Note the shear and the increase with time of the altitude at which the velocity changes sign.

What causes the velocity shear? One clue is the position within the F layer at which the transition from westward to eastward drifts occurs. We did not obtain F region density profiles during the interferometer experiments, but the rocket measurements referred to above indicate that the transition is near the very bottom of the F layer. This is the region in which, at night, control of the electric field passes from the E region dynamo to the F region dynamo. In the E region the electron densities at night are very low, but so are the densities in the 'valley' region above, and so the electric fields there are still strongly coupled along magnetic field lines to the E region north and south of the equator. For example, the altitude of 300 km at the dip equator is coupled to the E region at magnetic latitudes of approximately $\pm 10^{\circ}$. At latitudes below about 30° the E region zonal wind caused by the solar diurnal (1, -2) tidal mode is westward at night until about 0130 local time [e.g., Stening, 1969; Tarpley, 1970]. This wind will generate a northward and upward directed electric field in the E region which will map to an upward field in the F region, where it will produce a westward plasma drift, in agreement with our observations.

At higher altitudes, within the main F layer, the electron density is much larger than in the E region, and F region polarization fields generated by F region winds build up without being shorted out by the E region [Rishbeth, 1971]. These F region dynamo fields cause the plasma to drift at very nearly the velocity of the eastward F region neutral wind.

Heelis et al. [1974] have done some numerical calculations of equatorial drifts that include the effects of both the E and F region dynamos, and their results for the evening period do show a shear, with westward drifts reversing to eastward as altitude increases. The reversal altitude was 210 km, which is much lower than what we observed, but that is probably because the height of the F layer assumed for the calculations was unrealistically low. Unfortunately no ionograms for Jicamarca or Huancayo are available for the period shown in Figure 3, but at other days during the same month, values of h'F (the minimum observable F region virtual height) above 450 km were often observed, and much earlier studies of equatorial spread F have shown that the 'valley' region of very low electron densities always extends to altitudes of 300 km or more when spread F is observed [Farley et al., 1970].

The altitude of the observed velocity reversal, shown in Figure 3, increases initially with an apparent velocity of about 25 m/s, which is comparable to the evening vertical drift velocity. It is thus tempting to associate the two, but a careful study shows that there are differences. For example, the altitude of the drift reversal was increasing between 2025 and 2034 while the Doppler velocity was reversing from upward to downward. The difference is not really surprising since several variables which we have ignored in our simple explanation are involved in the coupling of the E and F region dynamos. An accurate model must include the effects of plasma transport and recombination in both regions, as well as the neutral wind behavior.

Conclusions

The radar interferometer technique shows great promise for studying the plasma processes associated with equatorial F region irregularities. Our first observations suggest that the echoes with broad multi-peaked Doppler spectra are associated with plasma 'bubble' walls, which in turn implies that sharp density gradients play an important role in generating the 3-meter wavelength irregularities responsible for the radar scatter. Profiles of the zonal plasma drift velocity during the evening showed a pronounced shear, with westward drifts in the lower F region and/or 'valley' region, and eastward drifts above. We believe that the westward drifts are driven by the E region dynamo and the eastward drifts by the F region dynamo.

Acknowledgments. We thank the staff of the Jicamarca Observatory for their help with the observations. The Observatory is operated by the Geophysical Institute of Peru, Ministry of Education, with support from the National Science Foundation and the National Aeronautics and Space Administration. This work was supported by the Aeronomy Program, Division of Atmospheric Sciences, of the National Science Foundation, through grant ATM78-12323.

References

Farley, D. T., B. B. Balsley, R. F. Woodman, and J. P. McClure, Equatorial spread F: Implications of VHF radar observations, J. Geophys. Res., 75, 7199, 1970.

Farley, D. T., H. M. Ierkic, and B. G. Fejer, Radar Interferometry: A new technique for studying plasma turbulence in the ionosphere, J. Geophys. Res., in press, 1981.

Fejer, B. G., D. T. Farley, C. A. Gonzales, R. F. Woodman, and C. Calderon, F-region east-west drifts at Jicamarca, J. Geophys. Res., 86, 215, 1981.

Heelis, R. A., P. C. Kendall, R. J. Moffett, and D. W. Windle, Electrical coupling of the E- and F-regions and its effect on F-region drifts and winds, Planet. Space Sci., 22, 743, 1974.

Ierkic, H. M., Radar observations of the equatorial electrojet irregularities and theory of type 1 turbulence, Ph.D. thesis, Cornell University, Ithaca, NY, 1980.

Rishbeth, H., Polarization fields produced by winds in the equatorial F-region, Planet. Space Sci., 19, 357, 1971.

Stening, R. J, An assessment of the contribution of various tidal winds to the Sq current system, Planet. Space Sci., 17, 889, 1969.

Tarpley, J. D., Ionospheric wind dynamo - II, Solar tides, Planet. Space Sci., 18, 1091, 1970.

Tsunoda, R. T., R. C. Livingston, and C. L. Rino, Evidence of a shear in bulk plasma motion associated with the post-sunset rise of the equatorial F layer, Geophys. Res. Lett., submitted, 1981.

Valenzuela, A., G. Haerendel, A. Foppl, H. Kappler, R. F. Woodman, B. G. Fejer, and M. C. Kelley, Barium cloud observations of shear flow in the post sunset equatorial F layer, Geophys. Res. Lett., to be submitted, 1981.

Woodman, R. F., East-west ionospheric drifts at the magnetic equator, Space Res., 12, 969, 1972.

Woodman, R. F., and C. LaHoz, Radar observations of F region equatorial irregularities, J. Geophys. Res., 81, 5447, 1976.

(Received January 5, 1981;
accepted February 20, 1981.)